Oceanization of the northern Neotethys: Geochemical evidence from ophiolitic mélange basalts within the…

Article *in* Lithos · April 2010

DOI: 10.1016/j.lithos.2010.01.007

CITATIONS
45

READS
76

3 authors:

M. Cemal Göncüoglu
Middle East Technical University
390 PUBLICATIONS **4,062** CITATIONS
SEE PROFILE

Kaan Sayit
Middle East Technical University
68 PUBLICATIONS **237** CITATIONS
SEE PROFILE

Ugur Kagan Tekin
Hacettepe University
137 PUBLICATIONS **1,069** CITATIONS
SEE PROFILE

Lithos 116 (2010) 175–187

Contents lists available at ScienceDirect

Lithos

journal homepage: www.elsevier.com/locate/lithos

Oceanization of the northern Neotethys: Geochemical evidence from ophiolitic melange basalts within the İzmir–Ankara suture belt, NW Turkey

M. Cemal Göncüoglu [a,*], Kaan Sayit [a], U. Kagan Tekin [b]

[a] Middle East Technical University, Department of Geological Engineering, 06531, Ankara, Turkey
[b] Hacettepe University, Department of Geological Engineering, 06800, Beytepe, Ankara, Turkey

ARTICLE INFO

Article history:
Received 13 August 2009
Accepted 12 January 2010
Available online 21 January 2010

Keywords:
E-MORB
Neotethys
Rifting
Izmir–Ankara Ocean
Late Carnian
Oceanic crust

ABSTRACT

The remnants of the Neotethyan Izmir–Ankara Ocean, the main branch of Neotethys in the eastern Mediterranean are represented by the Dagküplü Melange Complex in Central Sakarya, NW Turkey. It comprises several blocks or tectonic slices of pillow lavas, some of which include mudstones and radiolarian cherts as intra-pillow-fillings or interlayers. In the Igdecik area, a huge basaltic block has been studied in detail. Geochemical data reveal three distinct basalt types separated by sheared contacts. The first of these groups is an enriched mid-oceanic ridge basalt (E-MORB) type which is enriched in the most incompatible trace elements relative to normal MORB (N-NORB) in addition to having heavy rare earth elements (HREE) depletion, suggesting the influence of residual garnet in their mantle source region. The second is back-arc basin basalt (BABB) type with relatively depleted trace element compositions with respect to N-MORB together with a negative Nb anomaly, suggesting generation above an intra-oceanic subduction zone where partial melts are derived from a depleted (MORB-like) mantle. The final group is island-arc tholeiite (IAT) type, displaying the most depleted trace element abundances among the studied groups in addition to marked Nb depletion, reflecting intra-oceanic supra-subduction zone (SSZ) signatures similar to the BABB-type but requiring a depleted mantle source which has experienced a previous melt extraction. Combined with a previously ascribed Late Triassic age of Tekin et al. (2002) (221 Ma, Late Carnian; based on the radiolarian fauna found in a chert layer alternating with mudstones), the associated basalts with E-MORB-type geochemical signatures, suggest formation of oceanic crust as early as Late Carnian. This age is the oldest thus far obtained from the basalts of the Izmir–Ankara Ocean. This new data provides constraints on tectonic models for the opening the Izmir–Ankara Ocean and its relationship to other branches of the Neotethyan ocean in the Eastern Mediterranean area.

1. Introduction

Ophiolites provide a good oppurtunity to examine ancient pieces of oceanic lithosphere and they record important evidence regarding a number of tectono-magmatic events, including rift opening, subduction-related processes, intra-plate magmatism (e.g., Pearce et al., 1981; Alabaster et al., 1982). However, in suture zones marking the closure of an oceanic realm, ophiolites are found as "dismembered" melange bodies that have formed owing to mixing in an accretionary prism during accretion/obduction events. This is the case in the Eastern Mediterranean where intact ophiolite complexes along the main suture belts provide only limited information about the geological past of the related oceans. These sequences only represent a part of the respective ocean, because the main bulk of the oceanic lithosphere is often subducted or dismembered. Studying dismembered ophiolitic bodies in melanges requires detailed examination in terms of both structural and geochemical features, since a basaltic body appearing as a single block might actually consist of a series of tectonically stacked bodies. Thus, even a single block may carry important evidence inherited from a number of distinct tectono-magmatic settings. In the Izmir–Ankara branch of Neotethys, information on the evolution of the oceanic lithosphere is derived from the basaltic melange blocks, as almost no complete ophiolitic successions are known; the very few larger ophiolitic bodies that occur along the Izmir–Ankara suture belt in NW Anatolia (Fig. 1) only preserve parts of the oceanic crust. Moreover, their mantle rocks are extremely serpentinized. The lower- and mid-crustal rocks (cumulates and dyke-complexes) are incomplete and not as informative as their volcanic counterparts in terms of geochemical variations and tectono-magmatic evaluation. Another advantage of studying the volcanic portions of ophiolites is that they are frequently associated with oceanic sediments (mudstones and radiolarian cherts) that can be dated using paleontology, which is precise and less expensive than

* Corresponding author. Tel.: +90 3122102681; fax: +90 3122105750.
E-mail addresses: mcgoncu@metu.edu.tr (M.C. Göncüoglu), ksayit@metu.edu.tr (K. Sayit), uktekin@hacettepe.edu.tr (U.K. Tekin).

0024-4937/$ – see front matter © 2010 Elsevier B.V. All rights reserved.
doi:10.1016/j.lithos.2010.01.007

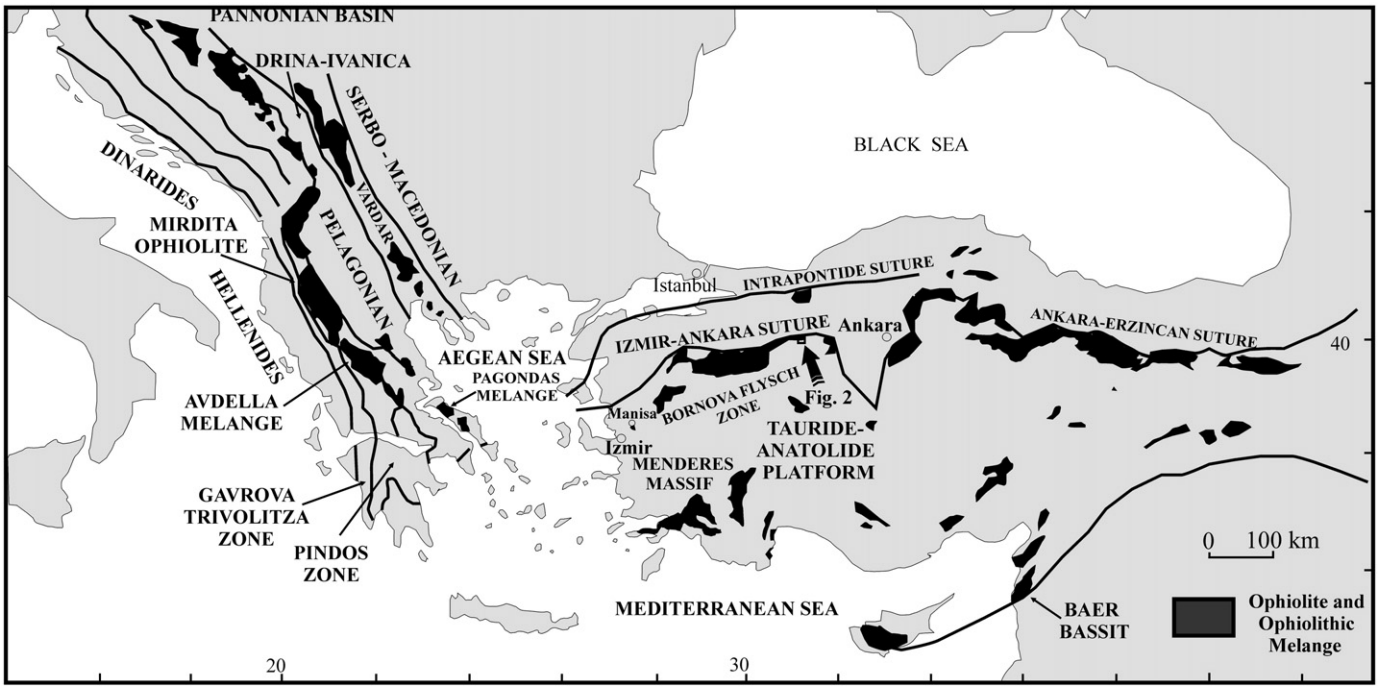

Fig. 1. Distribution of the Neotethyan oceanic branches and related suture belts in Balkan and the Eastern Mediterranean.

radiometric age dating methods (e.g. Göncüoglu et al., 2000, 2001, 2006a,b). The aim of this study is to understand the details and timing of the oceanic evolution, including basin opening and ridge-development, and its relation to the onset of subduction with associated back-arc and arc construction.

In this study we present the geochemical and petrological features of three tectonically associated basaltic successions that occur within a single block of 150 m size within the Central Sakarya ophiolitic melange of the Izmir–Ankara suture belt. In these basaltic successions, the E-MORB-type pillow basalts are interlayered with altering mudstone–chert sequences that yield late Carnian radiolarians (Tekin et al., 2002). This represents the oldest E-MORB-type basalt discovered thus far in the Izmir–Ankara Ocean and evidences a pre-late Carnian oceanic crust formation in the Neotethys, which was assumed to open during the Jurassic (e.g. Görür et al, 1983; Okay and Tüysüz, 1999). These new data will be discussed within the framework of the Neotethyan evolution in NW Turkey and its western continuation.

2. Regional geology

Izmir–Ankara Suture Belt represents the remnants of the Neotethys between the Tauride-Anatolide Platform in the south and the Sakarya Composite Terrane in the north. The suture can be followed eastwards for hundreds of kilometers towards Erzincan and into northern Iran. Towards the west, the Izmir–Ankara suture belt joins the Vardar suture on the opposite side of the Aegean Sea (Fig. 1).

Central Sakarya in NW Anatolia where the suture belt can be studied across a 10 km-long N–S geotraverse is one of the key areas for studying the Izmir–Ankara suture belt. The Anatolide Unit forms the lower tectonic block in the south. The subduction–accretion prism units of the Izmir–Ankara Ocean (Central Sakarya Ophiolitic Complex; Göncüoglu et al., 2000, 2006a) were thrust upon the Anatolide Unit along steep contacts. The oceanic relicts of the Izmir–Ankara Ocean, in turn, are overthrust by the uppermost tectonic unit, representing the basement rocks of the Sakarya Composite Terrane (Fig. 2).

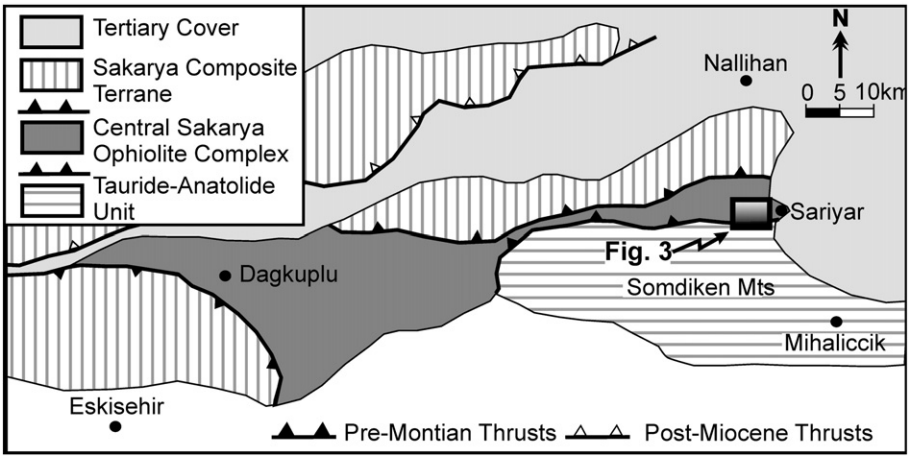

Fig. 2. Simplified map of the main structural units in the Central Sakarya area (after Göncüoglu et al., 2000).

The Anatolide Unit represents the metamorphic northern margin of the Gondwanan Tauride–Anatolide terrane. Its basement comprises orthogneisses, quartzofeldspathic schists, and garnet-bearing mica-schists with very rare carbonate and quartzite bands and greenschists with few lydite bands. Lithological equivalents of this unit occur in the south, in the Afyon area of Central Turkey and correspond to the Cadomian basement of the Tauride–Anatolide terrane (Gürsu and Göncüoglu, 2006). The disconformable overlying cover succession consists in its lower parts of quartzites and quartzite-recrystallized limestone bands, which are thought to be Middle Permian (Göncüoglu et al., 2000). The overlying Mesozoic succession starts with typical red continental clastics of Early Triassic and grades into a thick package of Mid Triassic to Late Jurassic–Early Cretaceous platformal limestones (Göncüoglu et al., 2003). Up-sequence, the succession is dominated by slope to basin-type pelagic cherty limestones and radiolarian cherts and grades into turbidites and olistostromes with ophiolitic detritus, thus recording to the emplacement of the Izmir–Ankara oceanic material on the Anatolide Passive margin (Göncüoglu and Türeli, 1993) The presence of *Globotruncana* sp. in the pelagic cherty limestones indicates that this emplacement is of Late Cretaceous age (Göncüoglu et al., 2000).

The Sakarya Composite Terrane represents the active margin of the Izmir–Ankara Ocean and consists of several tectonic units. The basement is made up of high-grade metaclastic and metabasic rocks intruded by Variscan granitoids. Locally preserved Permian platform-type deposits correspond to the first overstep sequence. The Early Triassic was characterized by extensional basin development, followed by the emplacement of oceanic material of Palaeotethys origin (The Karakaya Complex, e.g. Okay and Göncüoglu, 2004; Sayit and Göncüoglu, 2009) on this basinal succession, related to the Cimmerian events that characterize the closure of the Palaeotethys. Lower Jurassic to mid Cretaceous platform deposits unconformably overlie the Karakaya Complex as the second overstep sequence; they in turn are overlain by the oceanic assemblages from the northerly located Intra-Pontide branch of Neotethys during its Alpine closure.

The Central Sakarya Ophiolitic Complex, sandwiched between these two continental microplates or terranes, comprises an upper tectonic slice of more or less ordered ophiolite (The Tastepe Ophiolite) with sub-ophiolitic metamorphic rocks at its base and a lower, disrupted melange unit (Dagküplü Melange; Göncüoglu et al., 1997, 2000). The latter includes the Emremsultan Olistostrome and the Sariyar Tectonic Complex, the main topic of this paper. The Tastepe Ophiolite is almost 4 km thick and predominantly comprises slices of tectonites and mafic/to ultramafic cumulates. The Emremsultan Olistostrome is a block-in-matrix type allolistostrome with rare blocks of ophiolites and occurs mainly as a discrete tectonic sliver. It has a weakly deformed greywacke-dominated matrix. The Sariyar Tectonic Complex is a tectonic melange, dominated by sheared blocks and slivers of spilitic metabasalts, glaucophane–lawsonite schists, radiolarian cherts, pelagic limestones, serpentinites, and Mesozoic neritic limestones, some of which are a few kilometers across. Minor blocks are amphibolites, gabbros, pyroclastics and andesites/dacites. Locally, a sheared matrix of greywackes is found within the blocks.

The rocks re-evaluated in this paper are found in a megablock (Igdecik megablock) of Sariyar Tectonic Complex on the Igdecik road to the S–SW of the Sariyar Dam on the Sakarya River (Fig. 3) and dated by radiolarians (Göncüoglu et al., 2001; Tekin et al., 2002).

This megablock is about 1700 m thick and mainly includes massive and pillow basalts with ESE-dipping mudstone and chert interlayers (Fig. 4). Detailed petrographic and geochemical work reveals that the megablock comprises several tectonic slices, separated by second order internal thrusts. It is tectonically underlain by greywackes of the melange, which include up to 2 m long olistoliths of metabasaltic rocks with glaucophane, and gray and white recrystallized limestones and cherts.

The thickest slice is observed on both sides of the Igdecik road cut and consists of Group 1 (E-MORB-type, as defined in the geochemistry section) highly altered augite–phyric basalts (samples IGDE-1 and -3) with ca. 5 m-thick bands and irregularly shaped lenses of basaltic breccia. On the eastern escarpment of the Igdecik road an almost 20 m-thick sequence with red, thin to medium and occasionally thick-bedded (>1 m) limestones and cherts is found. Rare pink, carbonate-rich mudstone layers alternate with very fine-grained basalts and green to red mudstones (samples IGDE-4 and TO-25). From the uppermost part of this slice 1–2 cm thick radiolarite layers within the red limestone (sample 99-UKT-33) yielded early Late Carnian radiolarians (reported in detail by Tekin et al., 2002).

Group 2 massive and pillow lavas (BABB-type, as defined in the geochemistry section) with very thin pink carbonate lenses (samples IGDE-6, 7, 8, 9, 10 and TO-27) occur in the upper part of the section

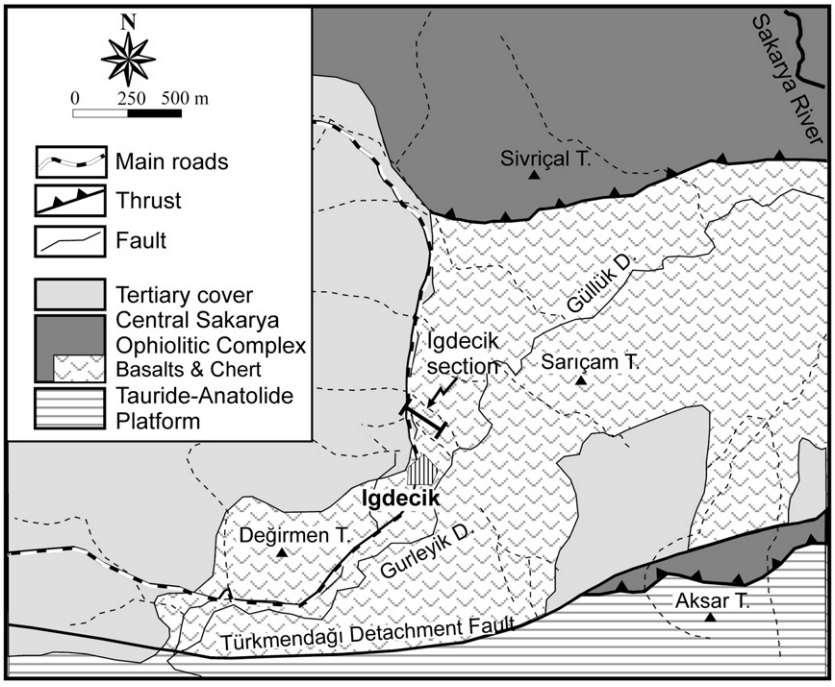

Fig. 3. The geological map of the Igdecik area and the location of the studied section (after Göncüoglu et al., 2001).

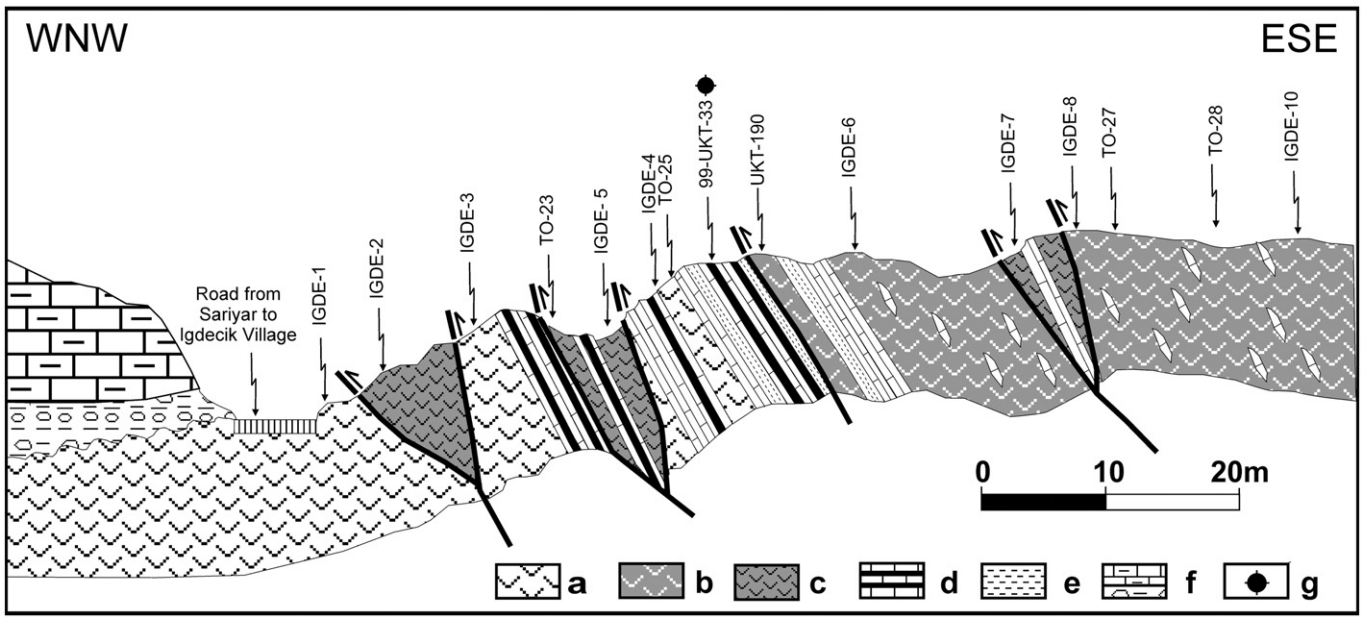

Fig. 4. Detailed cross-section of the studied succession and the location of the samples. Key to symbols: a. E-MORB-type basalts (Group 1), b. BABB-type basalts (Group 2), c. IAT-type basalts (Group 3), d. Alternation of red, thin to medium occasionally thick-bedded limestones and cherts, e. Green to red mudstones, f. Tertiary cover, and g. Radiolaria-bearing sample.

within the Igdecik megablock. The contacts between these slices are marked by highly sheared, green to red fault gouge of a few centimeters thick.

The Group 3 basalts (IAT-type, as defined in the geochemistry section) occur as three distinct tectonic slices, 5 to 7 m thick, within other lava packages along the section (Fig. 4, sample IGDE-2 within the lower part, IGDE-5 and TO-23 in the middle part and IGDE-7 in the upper part). They are also associated with rare carbonate-rich bands which have not yielded any fossils.

The oldest cover rocks unconformably overlying the Sariyar Tectonic Complex are of Early Paleocene–Early Eocene age. The Paleozoic and Mesozoic rock units of the Sakarya Composite Terrane tectonically overlie this Tertiary cover, indicating that the juxtaposition of Central Sakarya Ophiolitic Complex and the Late Cretaceous Sariyar Tectonic Complex is later than Early Eocene.

3. Petrography

The basalts investigated in this study have been variably affected by low-grade alteration as indicated by the secondary mineral assemblages that include albite, actinolite, chlorite, epidote and serpentine. Clinopyroxene is the only primary phase to have survived widespread alteration and it is generally observed as fractured crystals with poorly developed cleavages. It is replaced locally by actinolite, chlorite and epidote. In contrast to clinopyroxene, plagioclase feldspar appears to be strongly influenced by alteration such that it is totally replaced by secondary mineral phases. Albitization is common, and in some cases prehnite and actinolite are also observed as replacement minerals. All olivine crystals appear as pseudomorphs consisting largely of serpentine and chlorite and to a lesser extent actinolite. A mesh texture can be observed in some cases. The studied samples are mostly porphyritic; only a few samples are of aphyric appearance. Most of them are characterized by aphanitic basalts with phenocrysts of variable sizes embedded in a fine-grained groundmass, though a few coarse-grained diabasic varieties also exist. Glomeroporphyritic clusters are often present in the samples. Sub-ophitic texture is rarely observed. Some samples also show evidence of quenching with a glassy matrix totally altered by secondary products. Gas vesicles filled by secondary minerals, though not common, can be seen. These amygdales are observed to include prehnite, chlorite and quartz. Some samples include veins mostly made up of chlorite and calcite.

4. Geochemistry

The fourteen least-altered samples were selected for major and trace element geochemistry after detailed petrographic examination. Major elements in addition to Sc, Ba, and Ni were determined by inductively-coupled plasma atomic emission spectrometry (ICP-AES), whereas the rest of the trace elements including rare earth elements were analyzed by inductively-coupled plasma mass spectrometry (ICP-MS). All analyses were performed by ACME Analytical Laboratories Ltd. (Vancouver, Canada). The studied samples appear to have been influenced by low-grade hydrothermal alteration as indicated by large and variable loss on ignition values (LOI ≤ 7.4 wt.%). Some of major and trace elements are likely to have been remobilized, especially large ion lithophile elements (LILE) (e.g. Wood et al., 1976; Thompson, 1991). In contrast, the high field strength elements (HFSE) and REE are generally regarded to be relatively immobile during low-grade metamorphism (e.g. Pearce and Cann, 1973; Floyd and Winchester, 1978) and they can be used to place constraints on the primary geochemical features of the investigated rocks. It must be noted that all reported major element values have been normalized to 100% on a volatile-free basis for the following discussion. The whole-rock and trace element compositions of the Igdecik basalts are presented in Table 1. Analytical precision was generally better than 2% most of major elements and 3% for trace elements.

4.1. Classification

In order to provide a meaningful geochemical comparison, the investigated rocks were subdivided into three groups based on immobile incompatible element systematics. The studied basalts span a relatively large range of TiO_2 contents (0.36–1.55 wt.%), suggesting involvement of several mantle sources and/or a heterogeneous source and/or different degrees of partial melting for their generation. The relatively low Mg numbers between 43 and 67 [calculated as 100× atomic $Mg^{2+}/(Mg^{2+}+Fe^{2+})$; assuming that $Fe^{3+}/Fe^{2+}=0.15$] indicate that most of the Igdecik basalts have experienced fractional crystallization and do not represent primary magma compositions.

Table 1
Concentrations of the major, trace and rare earth elements for the Igdecik basalts (b.d.: below detections limits).

	E-MORB				IAT				BABB					
	TO-25	IGDE-1	IGDE-3	IGDE-4	TO-23	IGDE-2	IGDE-5	IGDE-7	TO-28	UKT-190	TO-27	IGDE-6	IGDE-8	IGDE-10
SiO_2	45.08	48.48	45.75	46.42	44.92	43.63	45.72	47.94	47.95	46.28	48.24	47.25	51.24	47.07
Al_2O_3	14.35	13.48	13.93	12.20	15.06	15.36	14.76	14.40	13.69	14.35	14.75	13.66	13.02	14.03
Fe_2O_3	10.82	10.14	10.76	9.94	9.24	10.98	8.86	9.42	11.31	10.39	10.91	12.09	11.36	12.18
MgO	5.92	3.35	6.79	7.29	5.45	5.07	7.78	8.45	7.16	7.02	5.98	7.13	7.07	6.02
CaO	11.41	15.43	13.06	12.99	14.57	15.35	13.71	11.84	10.64	12.03	10.25	10.77	9.44	11.27
Na_2O	1.39	1.63	2.21	1.77	2.32	2.40	1.48	1.69	1.84	1.79	2.07	2.40	1.60	1.69
K_2O	2.85	b.d.	0.60	0.11	0.31	0.05	0.23	0.35	0.57	0.62	1.14	0.20	0.23	0.22
TiO_2	1.45	1.26	1.36	1.35	0.33	0.58	0.32	0.48	0.78	0.58	0.73	0.64	0.79	0.76
P_2O_5	0.15	0.14	0.15	0.20	0.03	0.07	0.04	0.08	0.07	0.03	0.07	0.08	0.08	0.10
MnO	0.24	0.14	0.21	0.18	0.23	0.14	0.28	0.17	0.12	0.12	0.13	0.15	0.17	0.25
Cr_2O_3	0.061	0.097	0.067	0.117	0.131	0.063	0.104	0.075	0.043	0.031	0.024	0.035	0.051	0.068
LOI	6.6	5.8	5.1	7.4	7.0	6.3	6.7	5.1	5.4	6.5	5.6	5.6	4.9	6.3
Ni	116.0	90.8	105.6	211.8	163.0	82.7	141.1	95.3	71.0	74.0	64.0	61.7	93.9	102.1
Co	53.4	29.5	40.1	50.3	66.4	46.6	50.2	46.5	65.7	58.2	50.7	47.0	52.9	50.7
Sc	43	36	39	33	40	44	40	45	47	46	48	46	46	48
Ba	39.0	32.8	21.3	14.4	62.0	56.8	34.0	19.3	31.0	39.0	19.0	18.1	113.1	60.9
Pb	b.d.	0.5	0.7	0.9	b.d.	0.5	2.1	0.7	b.d.	b.d.	b.d.	0.4	0.2	0.3
Hf	2.5	2.0	2.2	2.7	0.7	1.0	0.5	0.9	1.6	0.8	1.1	1.0	1.1	1.3
Nb	10.7	8.6	9.7	15.5	0.6	1.3	0.5	1.6	3.5	1.8	3.8	3.2	3.6	3.5
Rb	40.1	1.0	11.1	1.6	4.5	0.9	2.7	5.9	13.6	15.8	17.7	4.4	4.0	4.6
Sr	65.3	55.5	78.8	89.4	115.3	51.4	64.9	55.6	58.6	64.0	97.1	42.5	62.0	29.0
Ta	1.1	0.5	0.6	0.9	b.d.	0.1	b.d.	0.2	0.3	b.d.	0.3	0.2	0.2	0.2
Th	1.0	1.3	0.6	1.6	0.1	0.4	0.1	0.3	0.5	0.4	0.7	0.3	0.4	0.4
U	0.8	0.2	0.4	0.4	0.2	0.1	0.1	0.2	b.d.	0.1	0.2	0.1	0.3	0.1
V	324	255	274	249	209	256	208	276	338	265	318	307	307	328
Zr	96.8	77.3	84.3	101.3	18.3	28.4	14.6	25.7	53.2	34.0	38.8	34.9	42.3	43.8
Y	26.7	19.7	21.5	21.4	14.0	16.7	12.8	16.1	22.7	19.8	20.3	19.4	20.0	21.6
La	10.1	7.3	8.0	11.8	0.9	1.4	0.9	1.8	2.8	2.0	2.7	2.6	2.5	3.3
Ce	21.8	15.9	17.6	24.1	1.7	3.4	1.2	2.7	6.7	4.6	6.7	5.3	6.4	6.1
Pr	3.1	2.29	2.55	3.29	0.33	0.68	0.26	0.47	1.07	0.76	0.92	0.82	0.9	1.08
Nd	15.2	11.0	12.2	16.1	2.3	4.2	1.7	2.8	6.0	3.9	5.4	4.4	5.4	6.2
Sm	3.8	2.6	2.9	3.4	0.9	1.1	0.6	1.0	2.0	1.8	1.8	1.4	1.5	1.8
Eu	1.48	0.93	1.04	1.12	0.41	0.51	0.34	0.42	0.78	0.60	0.64	0.50	0.56	0.65
Gd	4.42	3.05	3.25	3.74	1.49	1.96	1.35	1.76	2.86	2.34	2.54	2.06	2.29	2.58
Tb	0.70	0.58	0.69	0.67	0.31	0.43	0.29	0.39	0.55	0.43	0.45	0.43	0.52	0.54
Dy	5.07	3.61	3.94	3.81	2.50	2.94	2.17	2.53	3.96	3.30	3.58	3.18	3.28	3.51
Ho	1.11	0.73	0.78	0.74	0.60	0.60	0.47	0.57	0.94	0.77	0.83	0.65	0.72	0.78
Er	3.01	2.19	2.30	2.21	1.67	1.88	1.47	1.82	2.79	2.33	2.40	2.22	2.08	2.32
Tm	0.44	0.29	0.33	0.30	0.29	0.27	0.22	0.29	0.41	0.34	0.37	0.31	0.30	0.37
Yb	2.94	2.04	2.04	2.03	1.94	1.88	1.47	1.99	2.90	2.55	2.51	2.30	2.25	2.37
Lu	0.42	0.31	0.32	0.30	0.28	0.29	0.24	0.31	0.44	0.37	0.38	0.37	0.35	0.35

Using the chemical classification diagram of Winchester and Floyd (1977), the Igdecik basalts appear to be entirely sub-alkaline except for sample IGDE4 which straddles the alkaline boundary (Fig. 5). Group 1 samples display the highest Nb/Y values (0.40–0.72), whereas Group 2 and Group 3 basalts are characterized by lower values (0.09–0.19 and 0.04–0.10, respectively).

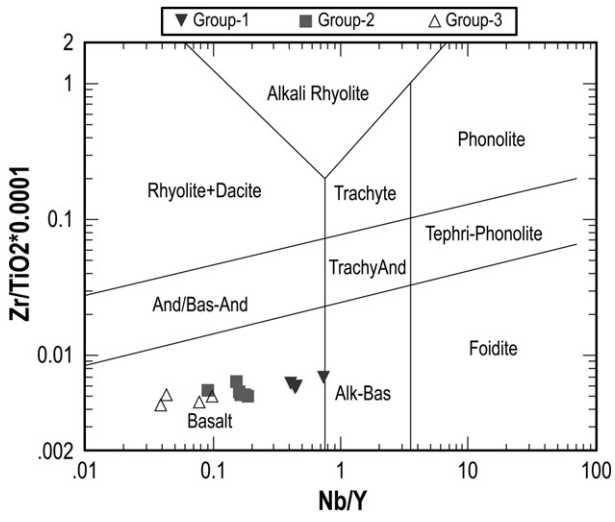

Fig. 5. Chemical classification of the Igdecik samples on the basis of immobile elements (after Winchester and Floyd, 1977).

4.2. Source features and variations

Group 1 basalts display the highest TiO_2 (1.34–1.55 wt.%), Nb (8.6–15.5 ppm) and Zr (77.3–101.3 ppm) concentrations, suggesting that their source region was more enriched and/or that they formed in response to smaller degree of melting (Fig. 6). Group 2 and 3 samples, however, show distinctly lower abundances of these elements, indicating generation from a more depleted source. This interpretation is supported by low Zr/Nb ratios of Group 1 (6.5–9.1), which are similar to those observed in E-MORB-type basalts (Zr/Nb = 8.8; Sun and McDonough, 1989). High Zr/Nb ratios in Group 2 and Group 3 samples (10.2–18.9 and 16.1–30.5, respectively) are more akin to N-MORB (Zr/Nb = 31.8; Sun and McDonough, 1989). It can be further suggested that the low Zr, Ti and Nb abundances as well as very high Zr/Nb ratios of Group 3 basalts may indicate that their source region has experienced a previous melt extraction from a MORB-like mantle source. Y/Nb values of Group 1 samples are also the lowest among the three (1.4–2.5), displaying similarities to enriched basaltic rocks (E-MORB- and OIB-type) from other Tethyan ophiolites (average $[Y/Nb]_{OIB} = 1.12$; $[Y/Nb]_{E\text{-}MORB} = 4.96$; compiled from Saccani and Photiades, 2005; Aldanmaz et al., 2008). Group 2 basalts have Y/Nb values between 5.4 and 11.0, while Group 3 displays the highest Y/Nb ratios (10.1–25.6) as expected from the significant Nb depletion seen in these basalts.

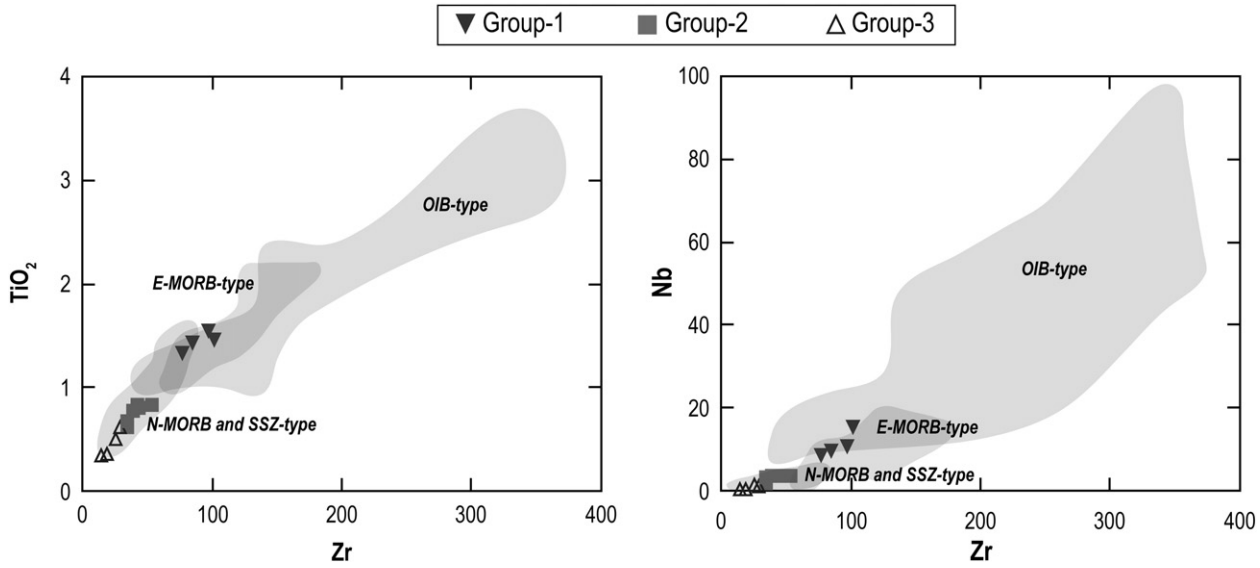

Fig. 6. Variations observed in TiO_2 and Nb against Zr display difference source features of the studied samples. Fields for the OIB-, E-MORB, N-MORB and SSZ-type Tethyan basaltic rocks are taken from Maheo et al. (2004), Saccani and Photiades (2005) and Aldanmaz et al. (2008).

The studied samples display largely consistent multi-element patterns for the immobile elements (HFSE and REE), indicating that the observed variations reflect primary igneous processes (Fig. 7). In contrast, LILE (except Th) shows scattered patterns likely resulting from hydrothermal alteration. Group 1 samples display variable enrichment in incompatible elements relative to N-MORB and are thus similar to E-MORB- and some OIB-type basalts erupted on within-plate settings or near spreading-centers (Weaver et al., 1987; Sun and McDonough, 1989; Baker et al., 1997; Haase et al., 1997; Furman et al., 2004). Group 2, however, shows variable enrichment in Th followed by depleted HFSE concentrations relative to N-MORB and slight negative Nb anomalies (Th/Nb = 0.09–0.22). Group 3 samples also have distinct Nb anomalies (Th/Nb = 0.17–0.31) and considerable depletion in HFSE compared to N-MORB. LILE enrichment together with variable depletion in HFSE is a typical feature characterizing magmas from subduction zones (Pearce, 1983; Peate et al., 1997; Gribble et al., 1998), which is assumed to result from modification of MORB-like mantle by aqueous fluids and melts coming from subducted oceanic slab (e.g. Gill, 1981; Hawkesworth et al., 1991; Pearce and Peate, 1995). The variable enrichment of Th relative to Nb, coupled with depleted HFSE concentrations therefore suggest that Groups 2 and 3 basalts may have been generated in an intra-oceanic subduction system.

Group-1 samples show slight fractionation from LREE to HREE ($[Ce/Yb]_N = 2.06–3.30$). It must be noted that sample IGDE-4 displays the highest LREE enrichment with La abundances reaching 50 times chondritic ($[La]_N = 49.79$, $[Ce]_N = 39.38$) and also has the most fractionated pattern within the group ($[Ce/Yb]_N = 3.30$). The other samples, however, show less fractionated REE patterns with $(Ce/Yb)_N$ between 2.06 and 2.40. The HREE fractionation relative to LREE observed in Group-1 samples suggests that garnet may have been a residual phase in their mantle source region and/or they have experienced small degrees of partial melting. In contrast, Group 2 is characterized by LREE-depleted patterns as indicated by low $(Ce/Yb)_N$ values (0.50–0.79). Group-3 is even more depleted in terms of LREE ($[Ce/Yb]_N = 0.23–0.50$). Such LREE-depleted patterns indicate that the mantle source of Groups 2 and 3 is more depleted than that of Group 1 and resembles an N-MORB-like source. The significantly depleted REE contents of the Group 3 basalts further suggest that their source region may have undergone a previous melt extraction event.

Variations in Ti/V further display the differences between the studied groups. Group-1 shows high Ti/V values (28.6–35.1), whereas Groups 2 and 3 display low ratios (13.2–16.2 and 9.9–14.5, respectively; Fig. 8). The low Ti/V ratios (<20) are suggestive of an arc signature (SSZ-type) (Shervais, 1982), consistent with their multi-element patterns. Note that although the Ti/V ratios of the two SSZ-type groups are similar to one other, Group-3 samples have with Y/Nb ratios, suggesting a similar (MORB-like) but more depleted source relative to that of Group 2, perhaps related to a previous melt extraction event as mentioned before.

The Ce/Y ratios of Group 1 samples are distinctly higher than those of basalts from Groups 2 and 3 (Fig. 9), which can be attributed to their derivation from a more enriched source and/or smaller degrees of partial melting. Indeed, Zr/Nb/Y systematics (Fig. 9) suggest that the compositional range of the E-MORB-like Group 1 basalts can be explained by two-component mixing of an enriched source (OIB-like) and a depleted source (N-MORB-like). Such a relationship can also be observed in modern MORB suites that have been influenced by mantle plumes, such as the Mid-Atlantic-Ridge, South American-Antarctic Ridge and Southwest Indian Ridge (Le Roex et al., 1983, 1985; Humpris et al., 1985). In contrast, the SSZ-type Groups 2 and 3 samples have lower Ce/Y and higher Zr/Nb values, thus indicating a dominant MORB-component in their genesis.

A Th/Yb-Nb/Yb plot (Fig. 10; Pearce and Peate, 1995) is particularly useful to identify source characteristics and subduction-related processes (Pearce, 1983), since Th and Nb reflect similar degrees of enrichment for within-plate processes, while subduction-related events and crustal contamination result in enrichment of Th but not Nb. Consequently, MORB and within-plate basalts with minimal crustal contribution fall within a region called the “MORB array”. Group 1 basalts plot in the MORB array except sample IGDE-1, indicating that most of these samples have not experienced crustal contamination and/or their mantle source region has not been previously fluxed by subduction components (Fig. 10). The slightly elevated Th/Yb of sample IGDE-1 suggests that it may have been modified by subduction enrichment or a crustal contaminant. It must be also noted that Group 1 samples are largely represented by compositions close to that of E-MORB proposed by Sun and McDonough (1989). The majority of Group 2 and all Group 3 samples, on the other hand, seem to have been variably influenced by subduction/crustal component. This result supports our interpretation that these samples have formed in a supra-subduction zone environment. This diagram also suggests that Group 1 samples are clearly of enriched compositions which may have been inherited, because either their mantle source region was geochemically enriched or they have been generated by very small degrees of partial melting.

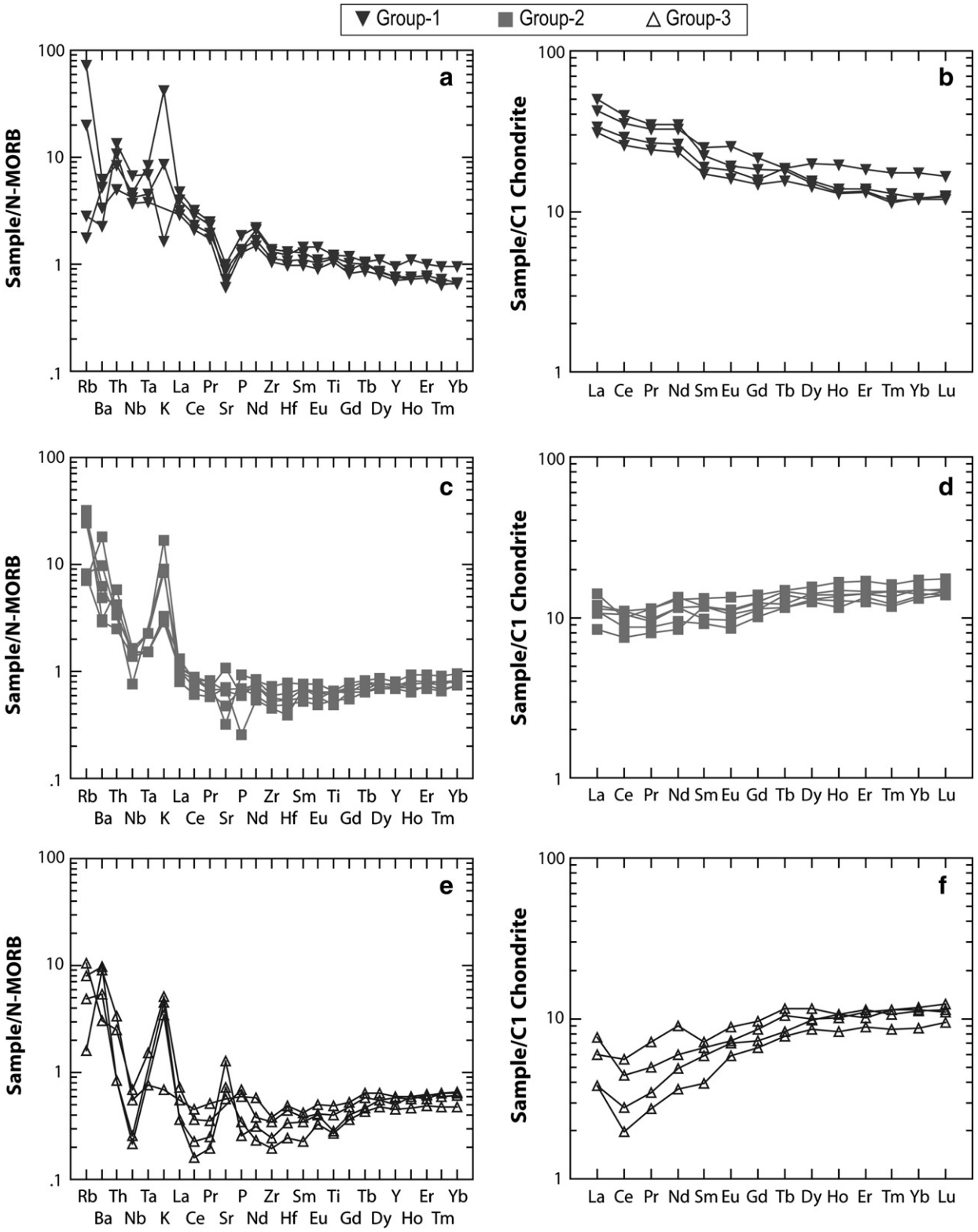

Fig. 7. Trace element and REE variations of the Igdecik basalts (normalization values for both N-MORB and C1-Chondrite from Sun and McDonough, 1989).

Basalts that have experienced minimal or no crustal contamination are characterized by high TiO_2/Yb ratios, since continental crust has relatively low Ti contents (Taylor and McLennan, 1995). Low TiO_2/Yb signatures, however, do not necessarily suggest the influence of crustal contamination. E-MORB-like Group-1 samples show moderate values ranging between 0.53 and 0.72, thus placing uncertainty about the effect of crustal contamination on these samples. In this respect, La/Nb and La/Ta ratios can be helpful. Basalts with low La/Nb (<1.5) and La/Ta (<22) are assumed to have suffered minimal crustal contamination (Hart et al., 1989; Saunders et al., 1992). Low ratios displayed by Group 1 basalts (La/Nb = 0.8–0.9, La/Ta = 9.2–14.6) therefore are indicative of minimal or no crustal contamination.

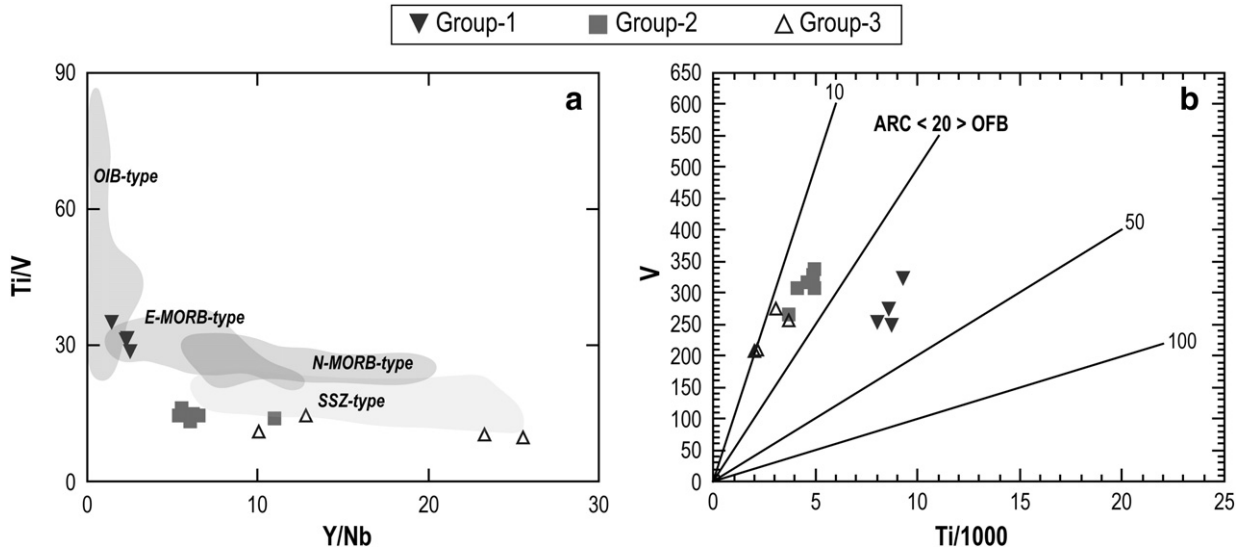

Fig. 8. a) Ti/V vs Y/Nb and b) Ti–V discrimination diagram (after Shervais 1982) for the Igdecik basalts. Data sources for the fields as in Fig. 6.

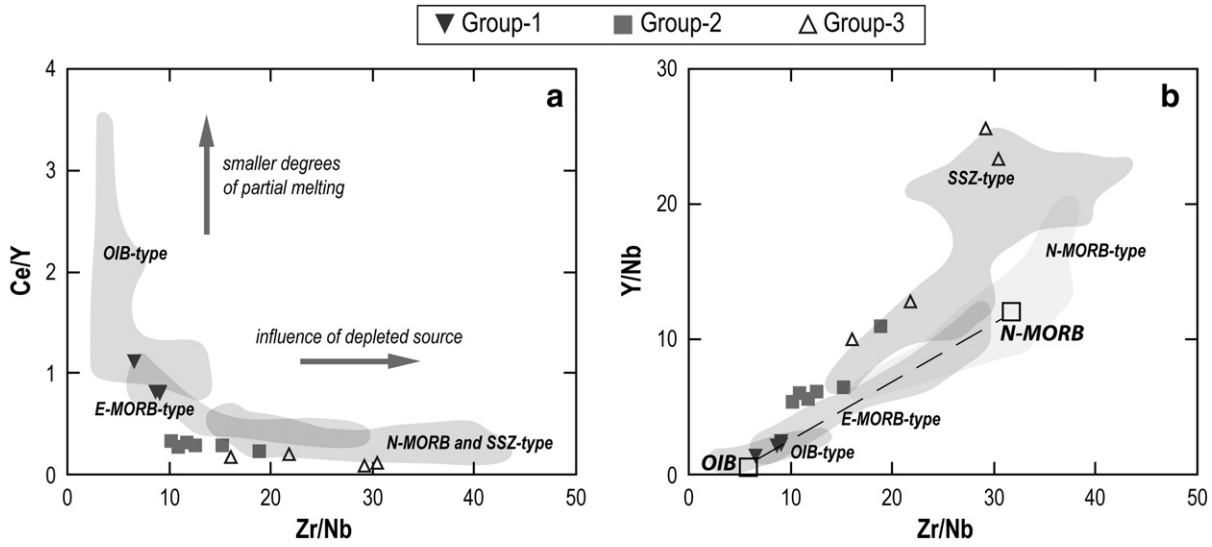

Fig. 9. Variation of Ce/Y and Y/Nb against Zr/Nb for the studied samples. N-MORB and OIB compositions are from Sun and McDonough (1989). Data sources for the fields as in Fig. 6.

Supporting this argument is the Th/Yb-Nb/Yb plot, where Group-1 samples fall along the mantle array defined by MORB- and OIB-type basalts that have experienced no crustal contamination.

4.3. Partial melting

In order to perform melt modeling of Group 1 samples, we used non-modal batch melting (Shaw, 1970) with distribution coefficients compiled from McKenzie and O'Nions (1991), Kelemen et al. (1993), Bedard (1994) and Johnson (1998) (Table 2). Concentrations of depleted and primitive mantle were taken from McKenzie and O'Nions (1991). We modeled partial melts on the basis of REE ratios, since they are sensitive to changes based on the presence of spinel or garnet in the mantle source. Fig. 11, shows that melts derived from a garnet–lherzolite source with a primitive mantle (PM) composition will generate melts with REE ratios that are too high for the investigated samples. However, 1.5%–3% partial melting of a mixed spinel–garnet-bearing source which is composed of 50% PM and 50% MORB source explains the composition of the Group 1 Igdecik basalts in both diagrams. Note that sample IGDE-4 requires smaller degrees

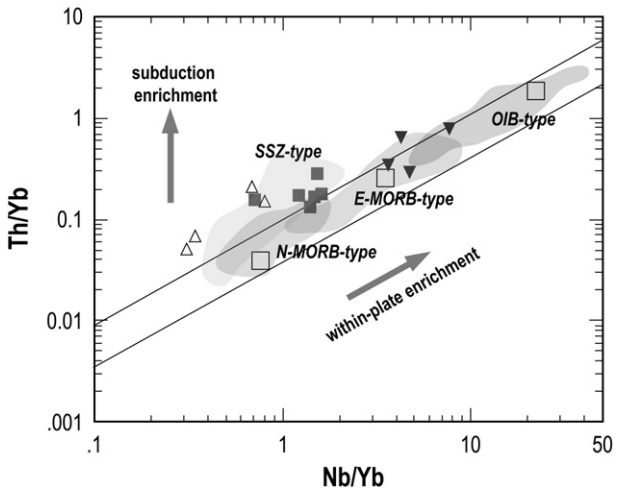

Fig. 10. Variation of Nb/Yb against Th/Yb on the Igdecik basalts (after Pearce and Peate, 1995). Compositions of N-MORB, E-MORB and OIB are from Sun and McDonough (1989). Data sources for the fields as in Fig. 6.

Table 2
Partition coefficients used in partial melting calculations and related references. (1) McKenzie and O'Nions (1991), (2) Kelemen et al. (1993), (3) Bedard (1994) and (4) Johnson (1998).

	Olivine	Ref	OPX	Ref	CPX	Ref	Garnet	Ref	Spinel	Ref
La	0.0004	1	0.0020	1	0.0536	2	0.0016	4	0.0100	1
Ce	0.0005	1	0.0030	1	0.0858	2	0.0050	4	0.0100	1
Pr	0.0008	1	0.0048	1	0.1500	1	0.0540	1	0.0100	1
Nd	0.0010	1	0.0068	1	0.1873	2	0.0520	4	0.0100	1
Sm	0.0013	1	0.0100	1	0.2910	2	0.5000	2	0.0100	1
Eu	0.0016	1	0.0130	1	0.3288	3	0.4000	4	0.0100	1
Gd	0.0015	1	0.0160	1	0.3670	3	2.0000	2	0.0100	1
Tb	0.0015	1	0.0190	1	0.4040	3	0.7500	1	0.0100	1
Dy	0.0017	1	0.0220	1	0.4420	2	2.2000	4	0.0100	1
Ho	0.0016	1	0.0260	1	0.4145	3	1.5300	1	0.0100	1
Er	0.0015	1	0.0300	1	0.3870	2	3.6000	4	0.0100	1
Tm	0.0015	1	0.0400	1	0.4085	3	3.0000	1	0.0100	1
Yb	0.0015	1	0.0490	1	0.4300	2	4.0300	1	0.0100	1
Lu	0.0015	1	0.0600	1	0.4330	3	5.5000	1	0.0100	1

of melting, which is in agreement with its more fractionated REE signature.

For the subduction-related samples, we used a Cr–Y plot (Fig. 12) of Murton (1989) that models incremental batch melting of an upper mantle lherzolite calculated on the basis of phase ratios given by Pearce (1980). The source S1 represents a MORB source, which gives way to the residue S2 after 20% partial melting; S3 refers to the residue formed after 12% partial melting of S2. This diagram suggests that the Group 2 (BABB-type) basalts can be modeled by approximately 40% of partial melting of an S1 source or, alternatively about 10% partial melting of an S2 source. Since 40% melting seems geologically unreasonable for the generation of SSZ-type magmas, the latter choice characterizing approximately 10% partial melt of a source that has previously experienced partial melting appears more appropriate. The Group 3 (IAT) samples, on the other hand, require larger degrees of melting (14–18%), in agreement with their extensively depleted nature as indicated by very low HFSE and LREE concentrations.

5. Tectono-magmatic evaluation

The Igdecik samples are all represented by sub-alkaline basalts (except sample IGDE-4 which is transitional to alkaline), and largely varying TiO_2 and Nb contents reflect a non-uniform origin for their generation. Indeed, trace element and REE variations reveal three distinct types: Group-1 (E-MORB-like), Group-2 (BABB-type), and Group-3 (IAT-type).

Group 1 basalts display variable enrichment in the most incompatible trace elements relative to N-MORB and show varying degrees of LREE enrichment together with slight depletion in HREE, which may be indicative of their derivation in the garnet stability field. Indeed, melt modeling based on REE ratios suggests that Group 1 Igdecik basalts require small amount of garnet (1.4%) in their mantle source in addition to spinel, thus suggesting their generation in the spinel–garnet transition

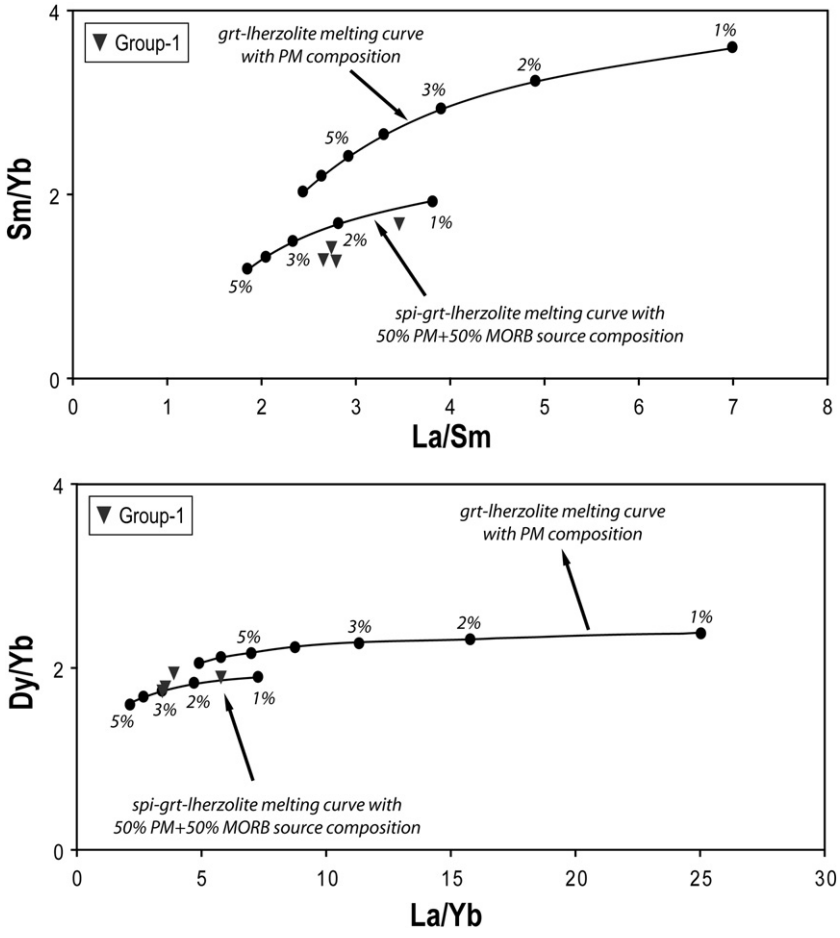

Fig. 11. Variation of La/Sm–Sm/Yb and La/Yb–Dy/Yb for the E-MORB-type Igdecik basalts. Melting paths are based on non-modal batch melting of a) garnet–lherzolite source of PM composition and b) spinel–garnet–lherzolite source with a composition of 50% PM and 50% DM. Garnet–lherzolite has a modal mineralogy of 0.60 oli + 0.20% opx + 0.14 cpx + 0.06 grt that melts in the proportions of 0.01 oli + 0.04 opx + 0.55 cpx + 0.40 grt (Haase et al., 1997). Spinel–garnet–lherzolite: 0.55 oli + 0.25 opx + 0.15 cpx + 0.014 grt, 0.03 spi that melts in the proportions of 0.05 oli + 0.05 opx + 0.30 cpx + 0.28 grt + 0.32 spi.

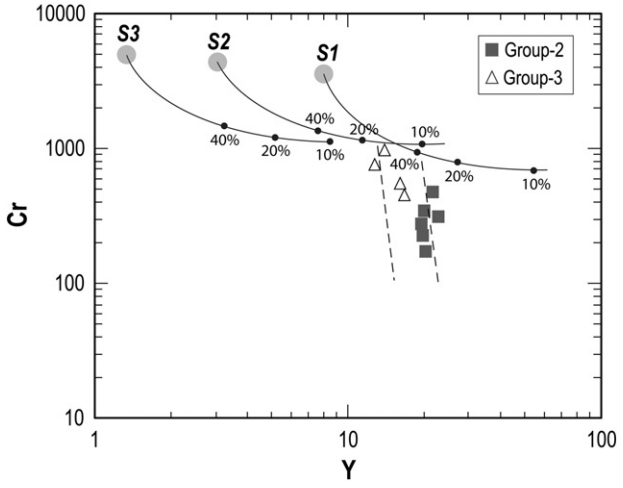

Fig. 12. Variation of Y vs Cr for the SSZ-type Igdecik basalts. Incremental batch melting curves and source compositions are based on Murton (1989). Melting paths represent non-modal incremental batch melting of a plagioclase-lherzolite source composed of 0.60 oli + 0.20 opx + 0.10 cpx + 0.10 plag that melts in the proportions of 3:1:4:4 respectively as given by Pearce (1980). S1 represents a MORB source that leads to the residue S2 after 20% partial melting, and S3 refers to the residue formed after 12% partial melting of S2.

field. E-MORB-type magmas can be generated in a variety of environments, such as at mid-oceanic ridges, back-arc basins, seamounts and oceanic islands, and continental rifts. The presence of pelagic sedimentary rocks, such as mudstones and cherts primarily associated with the submarine basalts, together with the Carnian (Upper Triassic) age acquired from one of the E-MORB-type suite (sample 99-UKT-33) suggest that these basalts can be interpreted (except for sample IGDE-1) to represent the initial stage of oceanic crust formation in a continental rift environment which may or may not be associated with a mantle plume (proto-oceanic stage). The absence of Upper Triassic N-MORB-type rocks in the succession (and in general from the Izmir–Ankara Suture Belt) reduces the possibility that the E-MORB-type basalts formed upon oceanic crust representative of a large ocean. Alternatively, these basalts may be of a seamount origin. The selection between these two alternatives is very difficult on geochemical grounds; however both cases require the development of oceanic crust. We do not, however, think that these basalts were formed at earlier stages of rifting (e.g. attenuated continental crust before oceanic spreading had begun), since there is no evidence for sub-aerial volcanics and shallow water deposition (e.g. neritic limestones). Supporting this argument is also the lack of alkali/transitional basalts and more evolved members (e.g. rhyolites, rhyodacites, and trachytes) typical of continental rift environments (e.g. Baker et al., 1977; Davies and MacDonald, 1987; Deniel et al., 1994; Peccerillo et al., 2003). Sample IGDE-1, however, may have been generated on a rift flank rather than above a spreading center. It is also possible that this sample could represent an older counterpart to the E-MORBs, perhaps recording magmatism on attenuated crust as suggested by its somewhat elevated Th/Nb ratios. These ratios may be indicative of crustal contamination and/or melting in a source region that have been modified by previous subduction-related events (a subcontinental lithospheric source).

A back-arc basin origin for Group 1 lavas seems unlikely, since that would imply both the initiation of a subduction system in the Upper Triassic and that the Neotethys Ocean had already started to close by that time. Therefore, E-MORB-type oceanic crust or a seamount origin appears the suitable tectonic setting.

Group 2 and especially Group 3 Igdecik basalts, in contrast to those from Group 1, show negative Nb anomalies but selective enrichment in Th, thus indicating an SSZ signature. The depleted nature of these basalts relative to N-MORB (as indicated by low HFSE abundances) suggests their generation in an intra-oceanic system. Group 2 samples show geochemical characteristics transitional between MORB and IAT, thus indicating that they may have been generated in a back-arc basin (extensional regime) rather than in an island-arc setting (e.g. Volpe et al., 1990; Pearce et al., 1995; Gribble et al., 1998). IAT-type Group 3 samples, however, display more depleted characteristics than Group 2 basalts, consistent with modeling that suggests a previous melt extraction from a MORB-like source. Since there is no age data available from these SSZ-type basalts, we can only say that these basalts imply an ongoing subduction in this part of Neotethys.

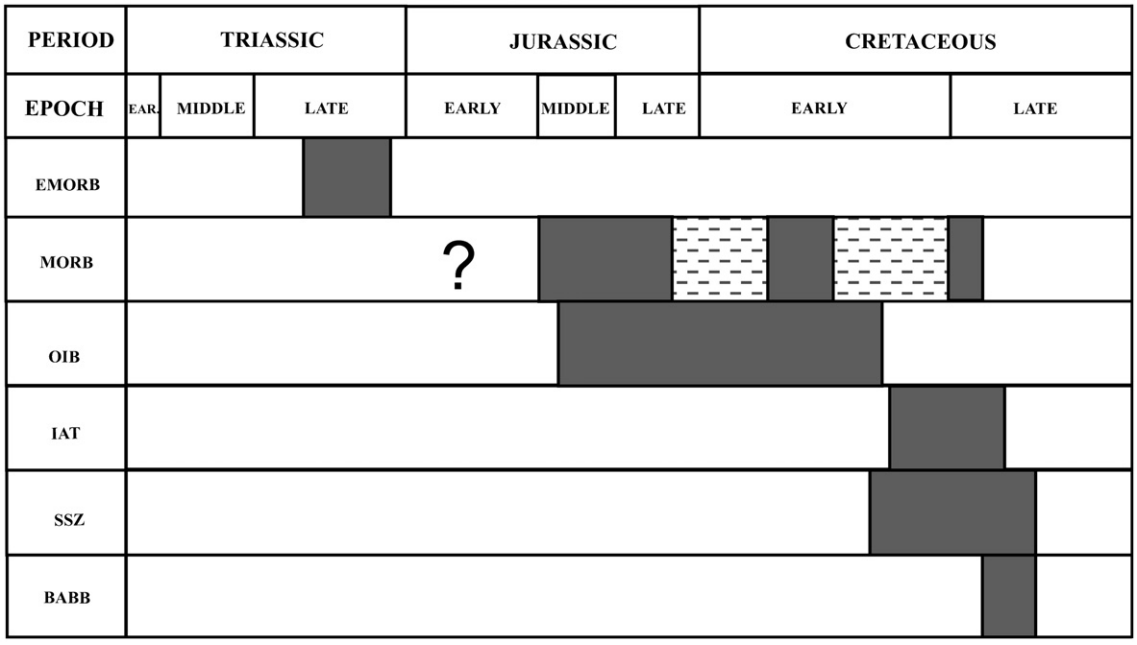

Fig. 13. Summary data on the tectono-magmatic type and radiolarian ages of oceanic basalts from the melange complexes within the Izmir–Ankara Suture Belt. Data from: Yaliniz et al, 1999, 2000; Göncüoglu et al, 2000, 2001; Tekin et al, 2002; Göncüoglu et al, 2003, 2006a,b; Tekin et al., 2006; Tekin and Göncüoglu, 2007; Göncüoglu et al., 2008; Tekin and Göncüoglu, 2009.

6. Evaluation in terms of a Neotethyan perspective

Although earlier work suggested that the Izmir–Ankara Suture Belt represents the relicts of one of the Neotethyan branches that opened during Early Liassic (Görür et al., 1983) more recent studies by Göncüoglu et al. (2003) and Tekin and Göncüoglu (2009) have argued that the rifting occurred during the Early Triassic. The evidence for a later rifting event is mainly the presence of rift-type Lower Triassic continental deposits and associated volcanism in the Anatolides (Gürsu and Göncüoglu, 2008). The recent discovery of radiolarian cherts of late Ladinian age (end of the Middle Triassic, Tekin and Göncüoglu, 2007) indicates the transitional period between rifting at the northern margin of the Tauride–Anatolide microcontinent and the formation of a deep (oceanic) basin. The discovery of basalts with E-MORB-type geochemical signatures in this study indicates that the formation of true oceanic crust may have taken place at Carnian time.

The ages, tectonic setting and life span of the oceanic volcanism within the Izmir–Ankara Ocean are summarized on Fig. 13. Our model, based on the data presented in this figure, suggests that the Early (?)-Mid Triassic rifting reached the stage of oceanic spreading during the Upper Triassic (Fig. 14a). The Middle–Late Jurassic OIB-type magmatism (Göncüoglu et al., 2000, 2006a,b, Rojay et al., 2001, Tekin and Göncüoglu, 2009) may well represent seamounts and oceanic islands fed by a mantle plume

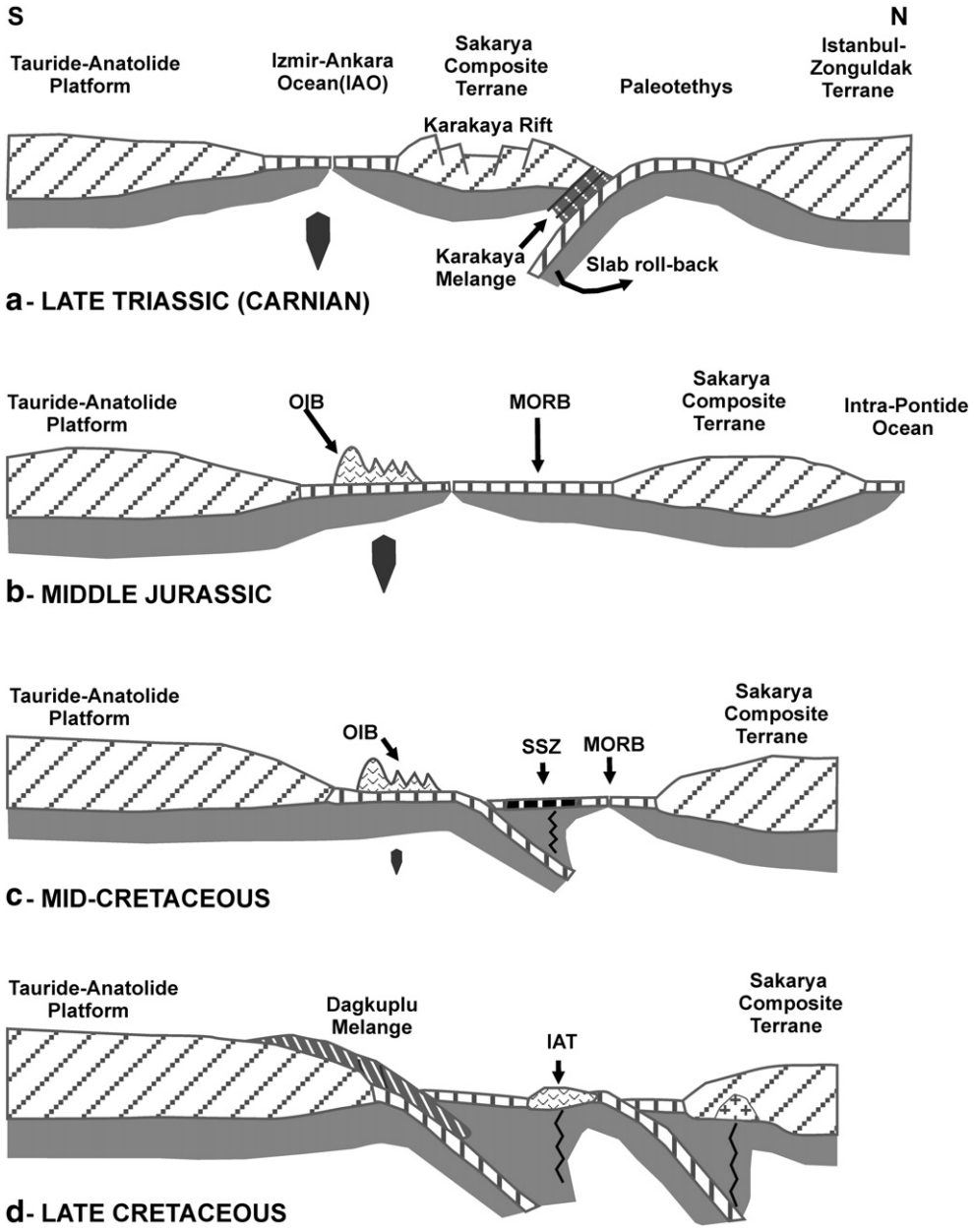

Fig. 14. Evolutionary cartoons for the geodynamic evolution of the Izmir–Ankara branch of Neotethys in NW Anatolia. a: The opening of the Izmir–Ankara Ocean began prior to Middle Carnian by slab-pull of the Paleotethyan oceanic lithosphere, giving way to extensional rift-basins within the Tauride-Anatolide platform. A northern seaway formed the Karakaya basin in the rifting Sakarya Composite terrane and the southern seaway developed to the Izmir–Ankara Ocean. The opening of the latter was triggered very probably by a plume that was active until Early Cretaceous. b: In general, Jurassic–Early Cretaceous is the period of ocean-spreading with formation of ocean islands (OIB). c: Starting in the mid Cretaceous, intra-oceanic decoupling by northward subduction began generating supra-subduction-zone (SSZ)-type oceanic crust with island arc (IAT), fore-and back-arc-type basaltic suites. d- During the late Late Cretaceous the double vergent-subduction was already controlling the closure of Izmir-Ankara Ocean, where subduction–accretion complexes forming the suture zone complexes (Dagkuplu Melange) of the Izmir–Ankara Suture Belt were generated.

formed on oceanic crust (Fig. 14b,c). In previous studies, this OIB-type magmatism is suggested to have continued from Middle–Late Jurassic to Early Cretaceous (Göncüoglu et al. 2000, 2006a,b). The onset of Late Triassic rifting discussed in this study may have resulted from the same mantle plume. Therefore the plume-related magmatism, described in this study, has lasted at least from Late Triassic to Early Cretaceous. Such a plume model is consistent with our present geochemical model which suggests a mixed mantle source consisting of both OIB-like and MORB-like domains for the generation of the E-MORB-type Igdecik basalts. The IAT- and BAB-type basalts described within the Igdecik megablock, on the other hand, provide further evidence for intra-oceanic subduction within the Izmir–Ankara Ocean (e.g. Göncüoglu et al., 1993; Floyd et al., 1998). Available data shows that this event started as early as late Early Cretaceous and continued up to Turonian time (Figs. 13, 14c,d).

The new geochemical data and our interpretation on Fig. 14 are not in accordance with some recent evolutionary models of the Neotethyan branches in the W Aegean and Anatolia (Moix et al., 2008). In these evolutionary models, Moix et al. (2008) suggest that the Izmir–Ankara Ocean did not open before the late Early Jurassic. They further suggest that the Izmir–Ankara suture actually includes two different melange complexes; one "north-directed diachronous Middle to Late Cretaceous melange obduction on the Jurassic Sakarya passive margin" and another "Senonian synchronous southward obduction on the Triassic passive margin" of Anatolides. They conclude "that the Izmir–Ankara suture, currently separating the Tauride–Anatolide and Sakarya microcontinents is composite, and that the passive margin of Sakarya is not the conjugate margin of the Anatolides". This interpretation requires two different oceans and extremely complex lateral displacements. Several lines of evidence argue against this interpretation. First, all structures in the Central Sakarya area are S-vergent (Göncüoglu et al., 2000), inconsistent with "north-directed ophiolite emplacement". Moreover, the ophiolites and ophiolite-bearing olistostromes on the Sakarya Composite Terrane are derived from the Intrapontide Ocean, which was located to the N of Sakarya (Göncüoglu et al., 2000, 2008; Robertson and Ustaömer, 2004). Second, there is no evidence for a northward subducting Huglu oceanic branch of the Izmir–Ankara Ocean during the Early Jurassic (Toarcian) or for a Phyrigian branch during the Early Cretaceous (Hauterivian) in the northern margin of the Anatolides. Detailed stratigraphic and structural data (Göncüoglu et al., 2000, 2003) from the Anatolide margin shows that during this period the platform-type deposition continued without any remarkable event indicating a "southward ophiolite obduction on the Triassic passive margin". Third, the juxtaposition age of the Karakaya Units and the Dagküplü Melange does not support the Moix et al. (2008) suggestion that "the lithologies older than Jurassic are likely derived from the Paleotethyan Karakaya Complex". As mentioned above, the Karakaya rocks were emplaced above the Paleocene–Eocene cover of the Dagküplü Melange, excluding a Late Cretaceous "merging of the two melanges".

Our new data and interpretation are in accordance with the data from the Balkan area (Papanikolaou, 2009; Robertson et al, 2009) across the Aegean Sea (Fig. 1). It is commonly accepted that the Neotethyan Vardar Ocean, the western continuation of the Izmir–Ankara Ocean in Greece and Serbia, had been rifted in Permo-Triassic (Sharp and Robertson, 2006) and the formation of the oceanic crust started already during Middle–Late Triassic time (Bortolotti et al, 2003; Karamata, 2006) as evidenced also by tectono-magmatic discrimination of basaltic rocks and paleontological ages of associated radiolarian cherts.

We suggest that the Late Carnian E-MORB-type rocks described in this study were formed in the early stages of the Izmir–Ankara Ocean and incorporated, together with pieces of MORB-, OIB- and SSZ-type oceanic crust into the subduction–accretion prism represented by the Dagküplü Melange of the Izmir–Ankara Suture Belt. This finding constitutes a reliable evidence for the geodynamic evolution of the northern Neotethys in a time period that spans Late Triassic–Upper Cretaceous and more information can be obtained by further studies on the ophiolitic melange basalts with known ages.

Acknowledgements

The authors gratefully acknowledge Necati Turhan for his contribution during the fieldwork in the Central Sakarya Area. The editor Andrew Kerr and two anonymous reviewers are thanked for their constructive comments on the manuscript. They would also like to thank Tanya Furman for her linguistic editing and helpful comments.

References

Alabaster, T., Pearce, J.A., Malpas, J., 1982. The volcanic stratigraphy and petrogenesis of the Oman ophiolite complex. Contributions to Mineralogy and Petrology 81, 168–183.
Aldanmaz, E., Yaliniz, M.K., Güctekin, A., Göncüoglu, M.C., 2008. Geochemical characteristics of mafic lavas from the Neotethyan ophiolites in western Turkey: implications for heterogeneous source contribution during variable stages of ocean crust generation. Geological Magazine 145, 37–54.
Baker, B.H., Goles, G.G., Leeman, W.P., Lindstrom, M.M., 1977. Geochemistry and petrogenesis of a basalt–benmoreite–trachyte suite from the southern part of the Gregory Rift, Kenya. Contributions to Mineralogy and Petrology 64, 303–332.
Baker, J.A., Menzies, M.A., Thirlwall, M.F., MacPherson, C.G., 1997. Petrogenesis of Quaternary intraplate volcanism, Sana'a, Yemen: implications for plume-lithosphere interaction and polybaric melt hybridization. Journal of Petrology 38, 1359–1390.
Bedard, J.H., 1994. A procedure for calculating the equilibrium distribution of trace elements among the minerals of cumulate rocks, and the concentration of trace elements in the coexisting liquids. Chemical Geology 118, 143–153.
Bortolotti, V., Carras, N., Chiari, M., Fazzuoli, M., Marcucci, M., Photiades, A., Principi, G., 2003. The Argolis Peninsula in the palaeogeographic and geodynamic frame of the Hellenides. Ofioliti 28, 79–94.
Davies, G.R., MacDonald, R., 1987. Crustal influences in the petrogenesis of the Naivasha basalt–rhyolite complex: combined trace element and Sr–Nd–Pb isotope constraints. Journal of Petrology 28, 1009–1031.
Deniel, C., Vidal, P., Coulon, C., Vellutini, P.-J., Piguet, P., 1994. Temporal evolution of mantle sources during continental rifting: the volcanism of Djibouti (Afar). Journal of Geophysical Research 99, 2853–2869.
Floyd, P.A., Winchester, J.A., 1978. Identification and discrimination of altered and metamorphosed volcanic rocks using immobile elements. Chemical Geology 21, 291–306.
Floyd, P.A., Yaliniz, M.K., Göncüoglu, M.C., 1998. Geochemistry and petrogenesis of intrusive and extrusive ophiolitic plagiogranites, Central Anatolian Crystalline Complex, Turkey. Lithos 42, 225–240.
Furman, T., Bryce, J.G., Karson, J., Iotti, A., 2004. East African rift system (EARS) plume structure: insights from Quaternary mafic lavas of Turkana, Kenya. Journal of Petrology 45, 1069–1088.
Gill, J.B., 1981. Orogenic Andesites and Plate Tectonics. Springer, Berlin. 390 pp.
Göncüoglu, M.C., Türeli, K., 1993. Petrology of the Central Anatolian plagiogranites and their geodynamic interpretation (Aksaray-Turkey). Turkish Journal of Earth Sciences 2, 195–203.
Göncüoglu, M.C., Yaliniz, K., Tekeli, O., 1993. Petrologic features and structural setting of the Central Anatolian ophiolites. 25th Anniversary of Earth Sciences, Abstracts, pp. 17–18.
Göncüoglu, M.C., Dirik, K., Kozlu, H., 1997. Pre-Alpine and Alpine Terranes in Turkey: explanatory notes to the terrane map of Turkey. Annales Geologique de Pays Hellenique 37, 515–536.
Göncüoglu, M.C., Turhan, N., Senturk, K., Özcan, A., Uysal, S., 2000. A geotraverse across NW Turkey: tectonic units of the Central Sakarya region and their tectonic evolution. In: Bozkurt, E., Winchester, J., Piper, J.A. (Eds.), Tectonics and Magmatism in Turkey and the Surrounding Area: Geological Society, London, Special Publications, vol. 173, pp. 139–161.
Göncüoglu, M.C., Tekin, U.K., Turhan, N., 2001. Geological implications of late Carnian radiolarian chert blocks within the Late Cretaceous Central Sakarya ophiolitic melange (NW Anatolia). Jeo 2000 Proceedings, CD-54-56. 6 pp.
Göncüoglu, M.C., Turhan, N., Tekin, K., 2003. Evidence for the Triassic rifting and opening of the Neotethyan Izmir-Ankara Ocean, northern edge of the Tauride-Anatolide Platform, Turkey. Bollettino della Societa Geologica Italiana Special Volmue 2, 203–212.
Göncüoglu, M.C., Yaliniz, K., Tekin, U.K., 2006a. Geochemistry, tectono-magmatic discrimination and radiolarian ages of basic extrusives within the Izmir-Ankara Suture Belt (NW Turkey): time constraints for the Neotethyan evolution. Ofioliti 31, 25–38.
Göncüoglu, M.C., Yaliniz, K., Tekin, U.K., 2006b. Geochemical features and radiolarian ages of volcanic rocks from the Izmir-Ankara Suture Belt, Western Turkey. Mesozoic Ophiolite Belts of the Northern Part of the Balkan Peninsula, Proceedings, pp. 41–44.
Göncüoglu, M.C., Gürsu, S., Tekin, U.K., Köksal, S., 2008. New data on the evolution of the Neotethyan oceanic branches in Turkey: Late Jurassic ridge spreading in the Intra-Pontide branch. Ofioliti 33, 153–164.
Görür, N., Sengör, A.M.C., Akkök, R., Yilmaz, Y., 1983. Pontidler'de Neo-Tetis'in kuzey kolunun açılmasına iliskin sedimentolojik veriler. Geological Bulletin of Turkey 26, 11–20.
Gribble, R.F., Stern, R.J., Newman, S., Bloomer, S.H., O'Hearn, T., 1998. Chemical and isotopic composition of lavas from the northern Mariana Trough; implications for magma genesis in back-arc basins. Journal of Petrology 39, 125–154.
Gürsu, S., Göncüoglu, M.C., 2006. Petrogenesis and tectonic setting of Late Pan-African meta-felsic rocks in Sandıklı area (Western Turkey). International Journal of Earth Sciences 95, 741–757.

Gürsu, S., Göncüoglu, M.C., 2008. Petrogenesis and geodynamic evolution of the Late Neoproterozoic post-collisional felsic magmatism in NE Afyon area, Western Central Turkey. In: Ennih, N., Lie´Geois, J.-P. (Eds.), The Boundaries of the West African Craton. Geological Society, London, Special Publications, 297, pp. 409–431.
Haase, K.M., Stoffers, P., Garbe-Schönberg, C.D., 1997. The petrogenetic evolution of lavas from Easter Island and neighbouring seamounts, near-ridge hotspot volcanoes in the SE Pacific. Journal of Petrology 38, 785–813.
Hart, W.K., Wolde, Gabriel G., Walter, R.C., Mertzman, S.A., 1989. Basaltic volcanism in Ethiopia: constraints on continental rifting and mantle interactions. Journal of Geophysical Research 94, 7731–7748.
Hawkesworth, C.J., Hergt, J.M., Ellam, R.M., McDermott, F., 1991. Element fluxes associated with subduction related magmatism. Philosophical Transactions of the Royal Society 335, 393–405.
Humpris, S.E., Thompson, G., Schilling, J.G., Kingsley, R.A., 1985. Petrological and geochemical variations along the Mid-Atlantic Ridge between 46°S and 32°S: influence of the Tristan da Cunha mantle plume. Geochimica at Cosmochimica Acta 49, 1445–1464.
Johnson, K.T.M., 1998. Experimental determination of partition coefficients for rare earth and high-field-strength elements between clinopyroxene, garnet, and basaltic melt at high pressures. Contributions to Mineralogy and Petrology 133, 60–68.
Karamata, S., 2006. The geological development of the Balkan Peninsula related to the approach, collision and compression of Gondwanan and Eurasian units. In: Robertson, A.H.F., Mountrakis, D. (Eds.), Tectonic development of the Eastern Meditteranean Region: Geological Society, London, Special Publications, 260, pp. 155–178.
Kelemen, P.B., Shimizu, N., Dunn, T., 1993. Relative depletion of niobium in some arc magmas and the continental crust: partitioning of K, Nb, La and Ce during melt/rock reaction in the upper mantle. Earth and Planetary Science Letters 120, 111–134.
Le Roex, A.P., Dick, H.J.B., Erlank, A.J., Reid, A.M., Frey, F.A., Hart, S.R., 1983. Geochemistry, mineralogy and petrogenesis of lavas erupted along the southwest Indian Ridge between the Bouvet triple junction and 11 degrees East. Journal of Petrology 24, 267–318.
Le Roex, A.P., Dick, H.J.B., Reid, A.M., Frey, F.A., Erlank, A.J., Hart, S.R., 1985. Petrology and geochemistry of basalts from the American–Antarctic Ridge, Southern Ocean: implications for the westward influence of the Bouvet mantle plume. Contributions to Mineralogy and Petrology 90, 367–380.
Maheo, G., Bertrand, H., Guillot, S., Villa, I.M., Keller, F., Capiez, P., 2004. The South Ladakh ophiolites (NW Himalaya, India): an intra-oceanic tholeiitic arc origin with implication for the closure of the Neo-Tethys. Chemical Geology 203, 273–303.
McKenzie, D., O'Nions, R.K., 1991. Partial melt distributions from inversion of rare earth element concentrations. Journal of Petrology 32, 1021–1091.
Moix, P., Beccaletto, L., Kozur, H.W., Hochard, C., Rosselet, F., Stampfli, G.M., 2008. A new classification of the Turkish terranes and sutures and its implication for the Paleotectonic history of the region. Tectonophysics 451, 7–39.
Murton, B.J., 1989. Tectonic controls on boninite genesis. In: Saunders, A.D., Norry, M.J. (Eds.), Magmatism in the Ocean Basins: Geological Society, London, Special Publications, 42, pp. 347–377.
Okay, A.I., Göncüoglu, M.C., 2004. The Karakaya Complex: a review of data and concepts. Turkish Journal of Earth Sciences 13, 77–95.
Okay, A.I., Tüysüz, O., 1999. Tethyan sutures of northern Turkey. Geological Society, London, Special Publications 156, 475–515.
Papanikolaou, D., 2009. Timing of tectonic emplacement of the ophiolites and terrane paleogeography in the Hellenides. Lithos 108, 262–280.
Pearce, J.A., 1980. Geochemical evidence for the genesis and eruptive setting of lavas from Tethyan ophiolites. In: Panayiotou, A. (Ed.), Ophiolites, Proceedings International Ophiolite Symposium, Cyprus, 1979. The Geological Survey of Cyprus, Nicosia, pp. 261–272.
Pearce, J.A., 1983. The role of sub-continental lithosphere in magma genesis at active continental margins. In: Hawkesworth, C.J., Norry, M.J. (Eds.), Continental Basalts and Mantle Xenoliths. Shiva, Nantwich, pp. 230–249.
Pearce, J.A., Cann, J.R., 1973. Tectonic setting of basic volcanic rocks determined using trace element analyses. Earth and Planetary Science Letters 19, 290–300.
Pearce, J.A., Peate, D.W., 1995. Tectonic implications of the composition of volcanic arc magmas. Annual Review of Earth and Planetary Sciences 23, 251–285.
Pearce, J.A., Alabaster, T., Shelton, A.W., Searle, M.P., 1981. The Oman ophiolite as a Cretaceous arc-basin complex: evidence and implications. Philosophical Transactions of the Royal Society 300, 299–317.
Pearce, J.A., Ernewein, M., Bloomer, S.H., Parson, L.M., Murton, B.J., Johnson, L.E., 1995. Geochemistry of Lau Basin volcanic rocks: influence of ridge segmentation and arc proximity. In: Smellie, J.L. (Ed.), Volcanism Associated with Extension at Consuming Plate Margins: Geological Society, London, Special Publications, 81, pp. 53–75.
Peate, D.W., Pearce, J.A., Hawkesworth, C.J., Colley, H., Edwards, C.M.H., Hirose, K., 1997. Geochemical variations in Vanuatu arc lavas: the role of subducted material and a variable wedge composition. Journal of Petrology 38, 1331–1358.
Peccerillo, A., Barberio, M.R., Yirgu, G., Ayalew, D., Barbieri, M., Wu, T.W., 2003. Relationships between mafic and peralkaline silicic magmatism in continental rift settings: a petrological, geochemical and isotopic study of the Gedensa Volcano, Central Ethiophian Rift. Journal of Petrology 44, 2003–2032.
Robertson, A.H.F., Ustaömer, T., 2004. Tectonic evolution of the Intra-Pontide suture zone in the Armutlu Peninsula, NW Turkey. Tectonophysics 381, 175–209.
Robertson, A.H.F., Karamata, S., Saric, K., 2009. Ophiolites and related geology of the Balkan region, the Mesozoic ophiolite belts of the northern part of the Balkan Peninsula. Lithos 108, vii–x.
Rojay, B., Yaliniz, M.K., Altiner, D., 2001. Tectonic implications of some Cretaceous pillow basalts from the North Anatolian ophiolitic melange (Central Anatolia-Turkey) to the evolution of Neotethys. Turkish Journal of Earth Sciences 10, 93–102.
Saccani, E., Photiades, A., 2005. Petrogenesis and tectonomagmatic significance of volcanic and subvolcanic rocks in the Albanide–Hellenide ophiolitic mélanges. The Island Arc 14, 494–516.
Saunders, A.D., Storey, M., Kent, R.W., Norry, M.J., 1992. Consequences of plume–lithosphere interactions. In: Storey, B.C., Alabaster, T., Pankhurst, R.J. (Eds.), Magmatism and the Causes of Continental Break-up: Geological Society, London, Special Publications, vol. 68, pp. 41–60.
Sayit, K., Göncüoglu, M.C., 2009. Geochemical characteristics of the basic volcanic rocks within the Karakaya Complex: a review. Yerbilimleri 30, 181–191 (in Turkish with English abstract).
Sharp, I.R., Robertson, A.H.F., 2006. Tectonosedimentary Evolution of the Western Margin of the Mesozoic Vardar Ocean: Evidence from the Pelagonian and Almopias Zones, Northern Greece. In: Robertson, A.H.F., Mountrakis, D. (Eds.), Tectonic development of the Eastern Meditteranean Region: Geological Society, London, Special Publications, vol. 260, pp. 373–412.
Shaw, D.M., 1970. Trace element fractionation during anatexis. Geochimica at Cosmochimica Acta 34, 237–243.
Shervais, M., 1982. Ti–V plots and the petrogenesis of modern and ophiolitic lavas. Earth and Planetary Science Letters 59, 101–118.
Sun, S.S., McDonough, W.F., 1989. Chemical and isotopic systematics of oceanic basalts: implications for mantle composition and processes. In: Saunders, A.D., Norry, M.J. (Eds.), Magmatism in the Ocean Basins: Geological Society, London, Special Publications, vol. 42, pp. 313–345.
Taylor, S.R., McLennan, S.M., 1995. The Geochemical Evolution of Continental Crust. Reviews of Geophysics 33, 241–265.
Tekin, U.K., Göncüoglu, M.C., 2007. Discovery of the oldest (upper Ladinian to middle Carnian) radiolarian assemblages from the Bornova Flysch Zone in western Turkey: implications for the evolution of the Neotethyan Izmir–Ankara Ocean. Ofioliti 32, 131–150.
Tekin, U.K., Göncüoglu, M.C., 2009. Late Middle Jurassic (Late Bathonian–Early Callovian) radiolarian cherts from the Neotethyan Bornova Flysch Zone, Spil Mountains, Western Turkey. Stratigraphy and Geological Correlation 17 (3), 298–308.
Tekin, U.K., Göncüoglu, M.C., Turhan, N., 2002. First evidence of Late Carnian radiolarian fauna from the Izmir–Ankara Suture Complex, Central Sakarya, Turkey: implications for the opening age of the Izmir–Ankara branch of Neotethys. Geobios 35, 127–135.
Tekin, U.K., Göncüoglu, M.C., Yaliniz, M.K., Altıner-Özkan, S., 2006. Dating of the Neotethyan volcanism by planktonic fossils (radiolaria and planktonic foraminifera) in the Bornova Flysch Zone, NW Turkey. TUBITAK 103Y027 Final Report. 229 pp.
Thompson, G., 1991. Metamorphic and hydrothermal processes: basalt-seawater interactions. In: Floyd, P.A. (Ed.), Oceanic Basalts. Blackie, Glasgow, pp. 148–173.
Volpe, A.M., Macdougall, J.D., Lugmair, G.W., Hawkins, J.W., Lonsdale, P., 1990. Fine-scale isotopic variation in Mariana Trough basalts: evidence for heterogeneity and a recycled component in backarc basin mantle. Earth and Planetary Science Letters 100, 251–264.
Weaver, B.L., Wood, D.A., Tarney, J., Joron, J-L., 1987. Geochemistry of ocean island basalts from the South Atlantic: Ascension, Bouvet, St. Helena, Gough and Tristan da Cunha. In: Fitton, J.G., Upton, B.G.J. (Eds.), Alkaline Igneous Rocks: Geological Society, London, Special Publications, vol. 30, pp. 253–267.
Winchester, J.A., Floyd, P.A., 1977. Geochemical discrimination of different magma series and their differentiation products using immobile elements. Chemical Geology 20, 325–343.
Wood, D.A., Gibson, I.L., Thompson, R.N., 1976. Elemental mobility during zeolite facies metamorphism of the Tertiary basalts of eastern Iceland. Contributions to Mineralogy and Petrology 55, 241–254.
Yaliniz, M.K., Aydın, N.S., Göncüoğlu, M.C., Parlak, O., 1999. Terlemez quartz monzonite of The Central Anatolia (Aksaray-Sarikaraman): age, petrogenesis and geotectonic implications for ophiolite emplacement. Geological Journal 34, 233–242.
Yaliniz, M.K., Göncüoglu, M.C., Özkan-Altıner, S., 2000. Formation and emplacement ages of the SSZ-type Neotethyan ophiolites in Central Anatolia, Turkey: paleotectonic implications. Geological Journal 35, 53–68.